

Bifurcation search via feedback loop breaking in biochemical signaling pathways with time delay

Steffen Waldherr, David Dylus, and Frank Allgöwer

Institute for Systems Theory and Automatic Control, Universität
Stuttgart, Pfaffenwaldring 9, 70550 Stuttgart, Germany

This is the pre-peer-reviewed version of the following article:
“*S. Waldherr, D. Dylus, and F. Allgöwer. Bifurcation search via feedback loop breaking in biochemical signaling pathways with time delay. Asian Journal of Control, 13(5):691–700, September 2011*”,
which has been published in final form at
<http://onlinelibrary.wiley.com/doi/10.1002/asjc.383/full>.

Abstract

We develop a method to locate bifurcations in time delay systems with a potentially high-dimensional parameter space. It is based on the feedback loop breaking approach that we developed and applied earlier for bifurcation search in ordinary differential equations. The method is particularly suited for the analysis of biological networks, for example to determine which parameters are relevant for complex dynamical behavior in such networks. To illustrate the benefits that this approach yields for biological network analysis, we apply it to study the effect of parameter variations on oscillations in a model of the MAP kinase cascade with a time delay.

1 INTRODUCTION

A major goal of systems biology is to provide mathematical methods for the analysis of complex dynamical behavior in intracellular networks, such as metabolic networks, biochemical signaling systems, or gene regulatory networks [12]. The development of such analysis methods is made difficult by the large number of uncertain or only vaguely known parameters in these typically non-linear systems. Classical approaches to study the dynamical behavior are often only feasible for a very small number of parameters, restricting their application to very small modules which may only yield limited biological insight.

Established methods of numerical continuation for bifurcation analysis are limited to parameter variations along a single line in parameter space [7]. The application of these methods may yield valuable insight into the possible dynamical behavior of small biological networks, if this line can be chosen in a

reasonable way. However, information about a good choice of the search direction for bifurcations is often not available, thus hampering the application of bifurcation analysis methods to biological networks with many parameters. To overcome this problem, we have recently proposed a bifurcation search method based on feedback loop breaking, thus taking a control engineering perspective on the complex dynamical behavior in the system and its relation to the presence of feedback loops [11].

The topic of this paper is to generalize the method developed in [11] for time delay systems. Time delays appear frequently in intracellular networks, for example due to time-consuming processes such as gene transcription [9]. While time delays have been shown to not affect the dynamical network behavior in special classes of systems such as positive feedback systems [5], other networks are crucially affected by time delays [8]. Usually, if a time delay system is stable dependent on the delay, a critical time delay value can be found, for which a change in stability will occur. Methods exist to find this critical time delay value, under the premise that all the other parameters are known [1, 2, 13, 10].

The approach developed in this paper allows to characterize critical points in time delay systems with a potentially high-dimensional parameter space. In addition, it can be applied to construct an algorithm which allows to systematically search for bifurcations of a desired type in such systems. In this algorithm, both the system's parameters as well as the value of the time delay can be varied simultaneously in order to reach a bifurcation. This flexibility makes the approach particularly suited for the analysis of biochemical network models, where many parameters are uncertain and can in principle be varied during an evaluation of the possible types of dynamical behavior in the network.

The paper is structured as follows. In Section 2, we extend the feedback loop breaking approach to time delay systems. The main results are presented in Section 3: a characterization of critical points in time delay systems, and an algorithm to systematically search for such points. The application of this approach to models of biochemical signaling pathways with a time delay is illustrated in Section 4 with a MAPK cascade model.

2 PRELIMINARIES

2.1 Feedback loop breaking in time delay systems

We consider a non-linear system with a single time delay given by the system of delay differential equations

$$\dot{x}(t) = F(x(t), x(t - \tau), p), \quad (1)$$

with state variables $x \in \mathbb{R}^n$, the delayed state $x(t - \tau) \in \mathbb{R}^n$, time delay $\tau \in \mathbb{R}_+$, parameters $p \in \mathcal{P} \subset \mathbb{R}^m$ and vector field $F : \mathbb{R}^n \times \mathbb{R}^n \times \mathcal{P} \rightarrow \mathbb{R}^n$.

An important characteristic of the time delay system (1) is that equilibria, i.e. constant steady state solutions, can be computed independently of the time

delay τ . We denote by $(x, p) \in \mathbb{R}^n \times \mathcal{P}$ a state-parameter pair for system (1). A pair $\xi = (\bar{x}, p)$ for which

$$F(\bar{x}, \bar{x}, p) = 0 \quad (2)$$

holds is called an extended equilibrium of (1), giving rise to the constant steady state solution $x(t) = \bar{x}$. Moreover, let \mathcal{M} be a smooth connected m -dimensional manifold of extended equilibria in $\mathbb{R}^n \times \mathcal{P}$, i.e. \mathcal{M} can be characterized by the condition

$$\forall \xi \in \mathcal{M} : F(\bar{x}, \bar{x}, p) = 0. \quad (3)$$

For ease of notation, we also combine the extended equilibrium ξ and the time delay τ in the pair

$$\bar{\xi} = (\xi, \tau) \in \bar{\mathcal{M}} = \mathcal{M} \times \mathbb{R}_+. \quad (4)$$

We first introduce the notion of a feedback loop breaking for system (1) being considered as closed loop system.

Definition 1. A loop breaking for the system (1) is a pair (f, h) , where $f : \mathbb{R}^n \times \mathbb{R}^n \times \mathbb{R} \times \mathcal{P} \rightarrow \mathbb{R}^n$ is a smooth vector field and $h : \mathbb{R}^n \times \mathbb{R}^n \rightarrow \mathbb{R}$ is a smooth function, such that

$$F(x, x_\tau, p) = f(x, x_\tau, h(x, x_\tau), p). \quad (5)$$

Thereby, we associate to (1) the open loop system

$$\begin{aligned} \dot{x}(t) &= f(x(t), x(t - \tau), u(t), p) \\ y(t) &= h(x(t), x(t - \tau)). \end{aligned} \quad (6)$$

The local dynamical properties of the system around equilibria are completely characterized by the linear approximation around these equilibria. In the next step, we therefore consider the linear approximation to the open loop system (6) in the neighborhood of an extended equilibrium $\xi = (\bar{x}, p) \in \mathcal{M}$. As a short hand notation, let $\bar{u} = h(\bar{x}, \bar{x})$.

Proposition 1. The linear approximation for the open loop system (6) in the neighborhood of the equilibrium-parameter pair $\xi \in \mathcal{M}$ is given by

$$\begin{aligned} \dot{z}(t) &= A(\xi)z(t) + A_\tau(\xi)z(t - \tau) + B(\xi)u(t) \\ w(t) &= C(\xi)z(t) + C_\tau(\xi)z(t - \tau), \end{aligned} \quad (7)$$

with $A(\xi) = \frac{\partial f}{\partial x}(\bar{x}, \bar{x}, \bar{u}, p)$, $A_\tau(\xi) = \frac{\partial f}{\partial x_\tau}(\bar{x}, \bar{x}, \bar{u}, p)$, $B(\xi) = \frac{\partial f}{\partial u}(\bar{x}, \bar{x}, \bar{u}, p)$, $C(\xi) = \frac{\partial h}{\partial x}(\bar{x}, \bar{x})$, and $C_\tau(\xi) = \frac{\partial h}{\partial x_\tau}(\bar{x}, \bar{x})$.

Then the linear approximation of the closed loop system (1) close to $\xi \in \mathcal{M}$ is given by

$$\begin{aligned} \dot{z}(t) &= (A(\xi) + B(\xi)C(\xi))z(t) + \\ &\quad (A_\tau(\xi) + B(\xi)C_\tau(\xi))z(t - \tau). \end{aligned} \quad (8)$$

2.2 Dynamical characterization of equilibria in the open and closed loop systems

The following analysis will be based on the loop transfer function $G(s) = \frac{W(s)}{U(s)}$, derived from a Laplace transformation of the linearized open loop system (7). From (7), the transfer function is computed as

$$G(\xi, \tau, s) = (C(\xi) + C_\tau(\xi)e^{-s\tau})(sI - A(\xi) - A_\tau(\xi)e^{-s\tau})^{-1}B(\xi). \quad (9)$$

In the following, we restrict the analysis to a less general class of time delay systems: assume that in the linearization (7) $C = 0$ and $A_\tau = 0$. This will for example be the case if the time delay appears only in one expression within the vector field F , and the loop breaking is chosen at exactly that point.

With the considered restriction, the loop transfer function $G(\xi, \tau, s)$ simplifies to

$$\begin{aligned} G(\xi, \tau, s) &= C_\tau(\xi)e^{-s\tau}(sI - A(\xi))^{-1}B(\xi) \\ &= \frac{\det \begin{pmatrix} sI - A(\xi) & -B(\xi) \\ C_\tau(\xi)e^{-s\tau} & 0 \end{pmatrix}}{\det(sI - A(\xi))} \end{aligned} \quad (10)$$

Also, the linear approximation of the closed loop system, in the general case given by (8), then simplifies to

$$\dot{z}(t) = A(\xi)z(t) + B(\xi)C_\tau(\xi)z(t - \tau). \quad (11)$$

In the following, we denote $D_\tau(\xi) = B(\xi)C_\tau(\xi)$.

As a preliminary result which will prove crucial for the main results, we provide a characterization of the closed loop poles in relation to the open loop transfer function $G(\xi, \tau, s)$ (10). Note that, for a time delay system, the poles of the closed loop are determined by the solutions of the quasipolynomial

$$\det(sI - A(\xi) - D_\tau(\xi)e^{-\tau s}) = 0, \quad (12)$$

which has infinitely many solutions for $\tau > 0$. Then, the poles of the closed loop relate to the transfer function $G(\xi, \tau, s)$ as given by the following result.

Lemma 1. $s_0 \in \mathbb{C}$ is a solution of $\det(sI - A(\xi) - D_\tau(\xi)e^{-\tau s}) = 0$, if and only if one of the following conditions hold:

(i) s_0 is not an eigenvalue of $A(\xi)$ and $G(\xi, \tau, s_0) = 1$;

(ii) s_0 is an eigenvalue of $A(\xi)$ and $\det \begin{pmatrix} s_0I - A(\xi) & -B(\xi) \\ C_\tau(\xi)e^{-\tau s_0} & 0 \end{pmatrix} = 0$.

Proof. To proof Lemma 1, we make use of Schur's lemma. The closed loop description (11) can be represented through the Schur complement as follows:

$$\begin{aligned}\det(sI - A - D_\tau e^{-\tau s}) &= \det \begin{pmatrix} sI - A & B \\ Ce^{-\tau s} & 1 \end{pmatrix} \\ &= \det(sI - A) - \sum_{i=1}^n (-1)^{n+1+i} b_i \det \left(\begin{pmatrix} (sI - A)_{-i} \\ Ce^{-\tau s} \end{pmatrix} \right),\end{aligned}$$

where M_{-i} is the matrix M with the i -th row deleted. Likewise a description with a 0 instead of a 1 is

$$\begin{aligned}\det \begin{pmatrix} sI - A & -B \\ Ce^{-\tau s} & 0 \end{pmatrix} &= \\ \sum_{i=1}^n (-1)^{n+1+i} b_i \det \left(\begin{pmatrix} (sI - A)_{-i} \\ Ce^{-\tau s} \end{pmatrix} \right).\end{aligned}$$

Subsequently the last two equations adopted into each other results in

$$\begin{aligned}\det \begin{pmatrix} sI - A & B \\ Ce^{-\tau s} & 1 \end{pmatrix} &= \\ \det(sI - A) - \det \begin{pmatrix} sI - A & -B \\ Ce^{-\tau s} & 0 \end{pmatrix}.\end{aligned}\tag{13}$$

Finally, dividing by $\det(sI - A)$ results in

$$G(\xi, \tau, s) = 1 - \frac{\det(sI - A - D_\tau e^{-\tau s})}{\det(sI - A)}.$$

s_0 is a solution of the quasipolynomial of the closed loop if and only if $\det(sI - A - D_\tau e^{-\tau s}) = 0$. Under the condition that $\det(s_0 I - A) \neq 0$, we see that this is equivalent to

$$G(\xi, \tau, s) = 1.$$

If $\det(s_0 I - A) = 0$ and $\det \begin{pmatrix} sI - A & -B \\ Ce^{-\tau s} & 0 \end{pmatrix} = 0$ then one gets directly from equation (13)

$$\det(s_0 I - A - D_\tau e^{-\tau s_0}) = 0.$$

□

In the next step, we develop the notion of critical frequencies for a time delay system, already introduced in [11]. To this end, let us represent the transfer function $G(\xi, \tau, s)$ (10) as

$$G(\xi, \tau, s) = \frac{k(\xi)q(s, \xi)e^{-s\tau}}{r(s, \xi)},\tag{14}$$

where q and r are polynomials in s with coefficients which are functions of ξ .

Furthermore, we make the following assumptions on the transfer function $G(\xi, \tau, s)$.

Assumption 1. *The transfer function $G(\xi, \tau, \cdot)$ does not have poles or zeros on the imaginary axis for any $\xi \in \mathcal{M}$, i.e.*

$$\forall \xi \in \mathcal{M} \forall \omega \in \mathbb{R} : k(\xi)q(\xi, j\omega) \neq 0 \text{ and } r(\xi, j\omega) \neq 0. \quad (15)$$

In addition, the degrees of $q(\xi, s)$ and $r(\xi, s)$ in s are assumed to be constant with respect to $\xi \in \mathcal{M}$.

Assumption 1 is usually satisfied, since the loop breaking in (5) can often be chosen such that the open loop system does not undergo the considered change in dynamical behavior.

Definition 2. *Under Assumption 1, $\omega_c \in \mathbb{R}$ is said to be a critical frequency for the transfer function $G(\xi, \tau, s)$ if*

$$G(\xi, \tau, j\omega_c) \in \mathbb{R}. \quad (16)$$

For each specific ξ and τ , all critical frequencies are given by the solution of the equation

$$\text{Im}(q(\xi, j\omega_c)r(\xi, -j\omega_c)e^{-\tau j\omega_c}) = 0. \quad (17)$$

The solutions of (17) can be combined in a set $\Omega_c(\xi)$ with an infinite number of elements. This set is given by

$$\Omega_c(\xi, \tau) = \{\omega \in \mathbb{R} | \text{Im}(q(\xi, j\omega_c)r(\xi, -j\omega_c)e^{-\tau j\omega_c}) = 0\}. \quad (18)$$

In [11], minimality of the set Ω_c of critical frequencies was a central assumption for the succeeding analysis. In this work, since the number of elements in Ω_c is infinite for a time delay system, we have to rephrase this assumption. To this end, let us write the set Ω_c as

$$\Omega_c(\xi, \tau) = \{\dots, -\omega^{(2)}(\bar{\xi}), -\omega^{(1)}(\bar{\xi}), 0, \omega^{(1)}(\bar{\xi}), \omega^{(2)}(\bar{\xi}), \dots\}, \quad (19)$$

where the $\omega_c^{(i)}(\bar{\xi})$ are continuous solution branches of the quasi-polynomial (17). We then have the following assumption, which can be seen as the analogue of the minimality assumption on Ω_c in [11].

Assumption 2. *The solution branches $\omega_c^{(i)}(\bar{\xi})$, $i \geq 1$, in (19) can be ordered such that, for any $\bar{\xi} \in \bar{\mathcal{M}}$,*

$$0 \leq \omega_c^{(1)}(\bar{\xi}) \leq \omega_c^{(2)}(\bar{\xi}) \leq \dots, \quad (20)$$

and, for any $i \geq 1$,

$$G(\xi, \tau, j\omega_c^{(i)}(\xi, \tau)) G(\xi, \tau, j\omega_c^{(i+1)}(\xi, \tau)) < 0. \quad (21)$$

3 MAIN RESULTS

3.1 Topological equivalence of equilibria

The main focus of this work is to establish criteria for a change in the dynamical properties of the considered system by varying parameters and the time delay. Such a change typically occurs at a critical point in state-parameter space, which is defined as follows.

Definition 3. *The extended equilibrium-delay pair $\bar{\xi}_c = (\xi_c, \tau_c) \in \bar{\mathcal{M}}$ is said to be a critical point for the system (1), if there exists $\omega_c \in \mathbb{R}$ such that $\det(sI - A(\xi_c) - D_\tau(\xi_c)e^{-\tau_c s}) = 0$, i.e. $j\omega_c$ is a pole of the linearized system at $\bar{\xi}_c$.*

A classical concept to study changes in the dynamical properties is via topological equivalence of equilibria [7]. A crucial result for time delay system in this respect is that the number of eigenvalues with positive real parts is finite [6]. Based on this result, topological equivalence in time delay systems can be defined as follows.

Definition 4. *Let $\bar{\xi}_1, \bar{\xi}_2 \in \bar{\mathcal{M}}$ be two hyperbolic extended equilibrium-delay pairs of the system (1). $\bar{\xi}_1$ and $\bar{\xi}_2$ are said to be topologically equivalent, if the two characteristic polynomials $\det(sI - A(\xi_1) - D_\tau(\xi_1)e^{-\tau_1 s})$ and $\det(sI - A(\xi_2) - D_\tau(\xi_2)e^{-\tau_2 s})$ have the same number of roots with positive real part.*

The major goal in this work is to find two parameter vectors $\bar{\xi}_1$ and $\bar{\xi}_2$ which have different stability properties, and are not topologically equivalent. Due to the continuous dependence of eigenvalues on parameters, this can only happen when $\det(sI - A(\xi) - D_\tau(\xi)e^{-\tau s}) = 0$ has a solution on the imaginary axis for a critical point $\bar{\xi}_c \in \bar{\mathcal{M}}$. Now first the infinite set $\Omega_c(\bar{\xi})$ will be considered for one specific extended equilibrium-delay pair $\bar{\xi}$. Then the number $\beta(\bar{\xi})$ will be defined as the number of ω_c in $\Omega_c(\bar{\xi})$ such that $G(\bar{\xi}, j\omega_c) > 1$, i.e.

$$\beta(\bar{\xi}) = \text{card}\{\omega_c \in \Omega_c(\bar{\xi}) | G(\bar{\xi}, j\omega_c) > 1\}.$$

The number $\beta(\bar{\xi})$ is always finite, as seen in the proof of Theorem 1.

The following result is helpful in order to characterize topological equivalence of equilibria.

Lemma 2. *Under the assumptions of the Theorem 1, the winding number of the image of the Nyquist curve Γ under the transfer function $G(\xi_i, \tau_i, \cdot)$, $i = 1, 2$, around the point 1 is given by*

$$|\text{wn}(G(\xi_i, \tau_i, \Gamma), 1)| = \beta(\bar{\xi}_i) \quad (22)$$

Proof. Since the loop breaking assures that $G(\xi, \tau, j\infty) = G(\xi, \tau, -j\infty) = 0$ and considering Assumption 2, a cut of $G(\xi_i, \tau_i, \Gamma)$ to the right of the point 1 is preceded and followed by a cut of $G(\xi_i, \tau_i, \Gamma)$ with the negative real axis. Thus, each cut to the right of the point 1 corresponds to one winding of $G(\xi_i, \tau_i, \Gamma)$ around the point 1. \square

Lemma 3. *Under the assumptions of Theorem 1, it is*

$$\begin{aligned} & |\text{wn}(G(\xi_1, \tau_1, \Gamma), 1) - \text{wn}(G(\xi_2, \tau_2, \Gamma), 1)| = \\ & |\beta(\bar{\xi}_1) - \beta(\bar{\xi}_2)| \end{aligned}$$

Proof. From Assumption 1, the transfer functions $G(\bar{\xi}_1, \cdot)$ and $G(\bar{\xi}_2, \cdot)$ have the same number of zeros and poles in the left and right half plane. Thus, for the phase differences we have $\arg(G(\bar{\xi}_1, j\infty)) - \arg(G(\bar{\xi}_1, -j\infty)) = \arg(G(\bar{\xi}_2, j\infty)) - \arg(G(\bar{\xi}_2, -j\infty))$, and due to symmetry of the transfer function with respect to positive / negative frequencies, $\arg(G(\bar{\xi}_1, j\infty)) = \arg(G(\bar{\xi}_2, j\infty))$. This implies that the winding numbers $\text{wn}(G(\bar{\xi}_1, \Gamma), 1)$ and $\text{wn}(G(\bar{\xi}_2, \Gamma), 1)$ have the same sign and with Lemma 2 it is concluded, that $|\text{wn}(G(\bar{\xi}_1, \Gamma), 1) - \text{wn}(G(\bar{\xi}_2, \Gamma), 1)| = ||\text{wn}(G(\bar{\xi}_1, \Gamma), 1)| - |\text{wn}(G(\bar{\xi}_2, \Gamma), 1)|| = |\beta(\bar{\xi}_1) - \beta(\bar{\xi}_2)|$. \square

With the help of the preceding lemma, the main result on topological equivalence can now be proven.

Theorem 1. *Assume that Assumptions 1 and 2 are satisfied. Let $\bar{\xi}_1, \bar{\xi}_2 \in \bar{\mathcal{M}}$ be two hyperbolic extended equilibrium-delay pairs of (1). Then $\bar{\xi}_1$ and $\bar{\xi}_2$ are topologically equivalent, if and only if*

$$\beta(\bar{\xi}_1) = \beta(\bar{\xi}_2).$$

Proof. By Definition 4, topological equivalence of $\bar{\xi}_1$ and $\bar{\xi}_2$ is equivalent to the condition that the function $\det(sI - A(\xi_1) - D_\tau(\xi_1)e^{-\tau_1 s})$ and $\det(sI - A(\xi_2) - D_\tau(\xi_2)e^{-\tau_2 s})$ have the same number of solutions with positive real part. From the proof of Lemma 1, it is known that

$$G(\bar{\xi}, s) - 1 = \frac{\det(sI - A(\xi) - D_\tau(\xi)e^{-\tau s})}{\det(sI - A(\xi))}.$$

Using the Nyquist criterion taken from [6] it is

$$\text{wn}(G(\bar{\xi}, \Gamma), 1) = n_{ol}(\bar{\xi}) - n_{cl}(\bar{\xi})$$

where $n_{cl}(\bar{\xi})$ ($n_{ol}(\bar{\xi})$) is the number of solutions of $\det(sI - A(\xi) - D_\tau(\xi)e^{-\tau s})$ ($\det(sI - A(\xi))$) with positive real part. Since $n_{cl}(\bar{\xi})$ and $n_{ol}(\bar{\xi})$ are both finite also $\text{wn}(G(\bar{\xi}_1, \Gamma), 1)$ is finite. By assumption, $n_{ol}(\bar{\xi}_1) = n_{ol}(\bar{\xi}_2)$ and thus $\bar{\xi}_1$ and $\bar{\xi}_2$ are topologically equivalent if and only if

$$\text{wn}(G(\bar{\xi}_1, \Gamma), 1) = \text{wn}(G(\bar{\xi}_2, \Gamma), 1).$$

\square

3.2 Existence of marginally stable equilibria

In the next step, we apply the previous results on topological equivalence in order to characterize marginally stable equilibria, or critical points where dynamical properties may change. To this end, the value of $G(\xi, \tau, j\omega_c^{(i)}(\bar{\xi}))$ has to

cross the point 1 during the variation of parameters and the time delay. This is equivalent to searching a $\bar{\xi}_c$ at which the function $\det(sI - A(\xi_c) - D_\tau(\xi_c)e^{-\tau s})$ has solutions on the imaginary axis. The crucial point is to fix one critical frequency branch from the set $\Omega_c(\bar{\xi})$ which is to be considered in the analysis. Then, the following result on existence of critical points is obtained.

Theorem 2. *Assume that Assumptions 1 and 2 are satisfied. There exists a critical point $\bar{\xi}_c \in \bar{\mathcal{M}}$, if and only if there exist $\bar{\xi}_1, \bar{\xi}_2 \in \bar{\mathcal{M}}$, for one critical frequency branch $\omega_c^{(i)}(\bar{\xi})$, with*

$$G(\bar{\xi}_1, j\omega_c^{(i)}(\bar{\xi}_1)) \leq 1 \leq G(\bar{\xi}_2, j\omega_c^{(i)}(\bar{\xi}_2)). \quad (23)$$

In that case, $\pm j\omega_c^{(i)}(\bar{\xi}_c)$ is a solution of $\det(sI - A(\xi_c) - D_\tau(\xi_c)e^{-\tau c s}) = 0$.

Proof. By Lemma 1, Assumption 1 assures that a point $\bar{\xi}_c$ is critical if and only if $G(\bar{\xi}_c, j\omega_c^{(i)}(\bar{\xi}_c)) = 1$.

Necessity: Under the condition $G(\bar{\xi}_c, j\omega_c^{(i)}(\bar{\xi}_c)) = 1$, take $\bar{\xi}_1 = \bar{\xi}_2 = \bar{\xi}_c$ and (23) follows trivially.

Sufficiency: Let $\bar{\xi}_1$ and $\bar{\xi}_2$ be such that (23) holds. Connectivity of $\bar{\mathcal{M}}$ implies that there is a path from $\bar{\xi}_1$ to $\bar{\xi}_2$ in $\bar{\mathcal{M}}$. Continuity of the critical frequency $\omega_c^{(i)}$ and the transfer function coefficients results in continuity of $G(\bar{\xi}, j\omega_c^{(i)}(\bar{\xi}))$ with respect to $\bar{\xi}$. This implies the existence of $\bar{\xi}_c$ having $G(\bar{\xi}_c, j\omega_c^{(i)}(\bar{\xi}_c)) = 1$ along any path from $\bar{\xi}_1$ to $\bar{\xi}_2$. \square

Note that the critical point $\bar{\xi}_c$ in Theorem 2 is typically not unique: usually, there is a submanifold of critical points with dimension m in the $(m + 1)$ -dimensional manifold $\bar{\mathcal{M}}$. The bifurcations which can occur on the submanifold are generally of codimension one, where we distinguish two main types. One is the Hopf bifurcation, which occurs when the considered critical frequency is unequal to zero, and the other one is a saddle-node bifurcation, which occurs when the considered critical frequency is equal to zero.

3.3 Bifurcation search in time delay systems

The theory derived in the previous section will now be applied to develop an algorithm to find bifurcations in the system (1). As a starting point, we consider a starting parameter vector p_1 , a corresponding equilibrium \bar{x}_1 , and the time delay τ_1 given. These are combined in the extended equilibrium-delay pair $\bar{\xi}_1$. The starting equilibrium \bar{x}_1 is assumed to be hyperbolic, otherwise the search for parameters yielding different dynamical properties is usually trivial. Furthermore, the manifold $\bar{\mathcal{M}}$ is assumed to be defined by a nonlinear equation of the form $\varphi(\bar{\xi}) = 0$. Normally $\varphi = F$ can be taken directly, but sometimes modifications are necessary, e.g. to exclude some solutions if the equation $F(\bar{x}, p) = 0$ has multiple solutions.

Given $\bar{\xi}_1$, the goal is to find an extended equilibrium-delay pair $\bar{\xi}_2$ such that $\bar{\xi}_1$ and $\bar{\xi}_2$ are not topologically equivalent according to Definition 4. In this case, existence of a critical point ξ_c is guaranteed from Theorem 2, and such a

point can be found on any path from $\bar{\xi}_1$ to $\bar{\xi}_2$ in $\bar{\mathcal{M}}$ via classical continuation methods. By choosing the critical frequency branch $\omega_c^{(i)}$ to be considered in the algorithm, it is even possible to search specifically for either static bifurcations, corresponding to $\omega_c^{(i)} = 0$, or dynamic (Hopf) bifurcations, corresponding to $\omega_c^{(i)} > 0$. In order to put the problem in the framework developed in this paper, a loop breaking for the system (1) has to be defined.

In order to simplify notation, we will in the following denote the considered critical frequency branch as $\bar{\omega}_c = \omega_c^{(i)}(\bar{\xi})$. Also, define the transfer function value at the critical frequency as

$$\gamma(\bar{\xi}_1) = G(\bar{\xi}_1, j\omega_c^{(i)}(\bar{\xi}_1)). \quad (24)$$

In the next step, two cases have to be distinguished. These cases depend highly on the initial Nyquist plot, particularly when the Nyquist plot has a crossing of the real axis smaller than 1 for the considered critical frequency branch $\omega_c^{(i)}$:

- (1) If $\gamma(\bar{\xi}_1) < 1$, the algorithm searches a pair $\bar{\xi}_2 \in \bar{\mathcal{M}}$ leading to $\gamma(\bar{\xi}_2) > 1$.

And the other case is if the Nyquist plot shows a crossing of the real axis bigger than 1 for the considered critical frequency $\omega_c^{(i)}$:

- (2) If $\gamma(\bar{\xi}_1) > 1$, the algorithm searches a pair $\bar{\xi}_2 \in \bar{\mathcal{M}}$ leading to $\gamma(\bar{\xi}_2) < 1$.

In the case of a dynamical system with a time delay (1) also the term of *gradient-directed continuation method*, as in [11], is used to describe this method in an appropriate manner. Hereby, the continuation is used to stay on the manifold $\bar{\mathcal{M}}$. The continuation method has to be complemented with a gradient ascent or descent approach, because $\bar{\mathcal{M}}$ is $m + 1$ -dimensional with typically $m > 1$. Therefore the continuation alone is not sufficient to achieve the desired value for $\gamma(\bar{\xi}_2)$. How the algorithm works is detailed as follows.

(1) Initialization

- a.) Set $k := 0$ and $\bar{\xi}^{(k)} := \bar{\xi}_1$
- b.) Set initial critical frequency $\bar{\omega}_c^{(k)} := \omega_c^{(i)}(\bar{\xi}^{(k)})$
- c.) Choose numerical parameters:
 - * Minimal required change: $\Delta\gamma$
 - * Initial step size: $\delta^{(0)}$
 - * Minimal and maximal step size: δ_{min} and δ_{max}

(2) Prediction step

- a.) Compute the gradient of γ with respect to changes in $\bar{\xi}$:

$$\begin{aligned} \nabla\gamma(\bar{\xi}^{(k)}) &= \frac{\partial G}{\partial \xi}(\bar{\xi}^{(k)}, j\bar{\omega}_c^{(k)}(\bar{\xi}^{(k)})) + \\ &\frac{\partial G}{\partial \bar{\omega}_c^{(k)}} \frac{\partial \bar{\omega}_c^{(k)}}{\partial \xi}(\bar{\xi}^{(k)}, j\bar{\omega}_c^{(k)}(\bar{\xi}^{(k)})) \end{aligned} \quad (25)$$

Here $\bar{\omega}_c^{(k)}$ is computed through solving (17) for ω_c via a Newton Method and then used to compute $\nabla\gamma(\bar{\xi}^{(k)})$.

b.) Compute the tangent space to $\bar{\mathcal{M}}$ at $\bar{\xi}^{(k)}$:

$$T_{\bar{\xi}^{(k)}}\bar{\mathcal{M}} = \text{null} \frac{\partial \varphi}{\partial \xi}(\bar{\xi}^{(k)}) \quad (26)$$

c.) Project $\nabla\gamma(\bar{\xi}^{(k)})$ on $T_{\bar{\xi}^{(k)}}\bar{\mathcal{M}}$:

$$v^{(k)} = \text{Proj}(\nabla\gamma(\bar{\xi}^{(k)}), T_{\bar{\xi}^{(k)}}\bar{\mathcal{M}}) \quad (27)$$

d.) Set prediction point:

$$\bar{\xi}_{pre}^{(k+1)} = \bar{\xi}^{(k)} + \delta^{(k)} v^{(k)} \quad (28)$$

(3) **Stepsize control** If necessary, the stepsize $\delta^{(k)}$ is updated in order to assure that

$$\gamma(\bar{\xi}_{pre}^{(k+1)}) - \gamma(\bar{\xi}^{(k)}) \geq \Delta\gamma, \quad (29)$$

holds, to ensure the minimal required change $\Delta\gamma$ in the transfer function value. This is done in iteration with (2d). Furthermore, the step size is kept within the constraints $\delta_{min} \leq \delta^{(k)} \leq \delta_{max}$. If this is not feasible, the algorithm aborts with an error.

(4) **Correction step**

Generally $\bar{\xi}_{pre}^{(k+1)} \notin \bar{\mathcal{M}}$, therefore to achieve $\bar{\xi}^{(k+1)} \in \bar{\mathcal{M}}$ a correction step is required. This correction step is made by using the Gauss-Newton method to solve the following system of nonlinear equations:

$$\begin{aligned} 0 &= \varphi(\bar{\xi}^{(k+1)}) \\ \gamma(\bar{\xi}^{(k+1)}) &= \gamma(\bar{\xi}_{pre}^{(k+1)}) \\ 0 &= \text{Im}(q(\bar{\xi}^{(k+1)}, j\bar{\omega}_c^{(k+1)}) \\ &\quad r(\bar{\xi}^{(k+1)}, -j\bar{\omega}_c^{(k+1)})e^{-\tau j\bar{\omega}_c^{(k+1)}}) \end{aligned} \quad (30)$$

for $\bar{\xi}^{(k+1)}$ and $\bar{\omega}_c^{(k+1)}$. Here $(\bar{\xi}_{pre}^{(k+1)}, \bar{\omega}_c^{(k)})$ is used as the starting point for the Newton iteration. Now there are two possibilities:

a.) **Success**, the algorithm takes the solution of $\bar{\xi}^{(k+1)}$ and goes to (5).

b.) **Failed**, the algorithm reduces the stepsize $\delta^{(k)}$ and goes to (2d).

(5) **Finishing step**

If $\gamma(\bar{\xi}^{(k+1)}) > 1 \Rightarrow$ **success**, else increase the step index k and go to step (2).

Since the computation of the critical frequency cannot be done analytically and it is therefore necessary to have an initial value, for every new value of $\bar{\xi}^{(k+1)}$ the old critical frequency $\bar{\omega}_c^{(k)}$ as starting value for the Newton iteration has to be taken. The algorithm finishes its computation in a finite number of steps because of the defined upper bound of the stepsize and through condition (29).

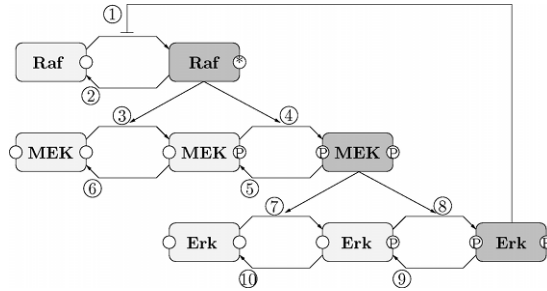


Figure 1: Schematic representation of the MAPK cascade.

4 ANALYSIS OF A MAPK SIGNALING CASCADE

As an example of how this algorithm helps to determine relevant parameter changes for a variation of the dynamical behavior of biochemical signaling networks, we will apply it to the search of a Hopf bifurcation in a model of the MAPK cascade with time delay. The MAPK cascade is one of the most intensively studied eukaryotic signaling pathways. It is at the heart of a molecular signaling network that governs the growth, proliferation, differentiation and survival of eukaryotic cells. In the last decade, the understanding of MAPK signaling was significantly enlarged by construction and analysis of mathematical models, e.g. [3, 4].

In this study, we will especially consider the MAPK cascade as it appears in the EGF (epidermal growth factor) receptor pathway. At the first level, the Raf compounds get activated by several mechanisms involving phosphorylation at a tyrosine residue. MEKs get activated at the second level by phosphorylated Raf and thus phosphorylated at serine and threonine residues. At the third level, the Erks are then activated by the MEKs and are phosphorylated at two sites, conserved threonine and tyrosine residues. Protein phosphatases inactivate the corresponding kinases at each cascade level. From the third layer, there is a negative feedback inhibiting SOS (son of sevenless homologue), which is required in the activation of Raf. A schematic description of the model is given in Figure 1. The mathematical model used here is proposed by [4], and has been adopted here with slight simplifications. In addition, since the inhibitory feedback from the third level of the cascade to the first involves several intermediate steps, we integrate a time delay in the corresponding phosphorylation reaction.

The goal of the analysis is to determine which parametric changes may lead to a change between non-oscillatory and oscillatory behavior. To this end, a suitable loop breaking point is defined, and the analysis method developed in the previous section is applied to the model.

4.1 Mathematical model for the MAPK cascade with time delay

In this section, we describe the mathematical model for the MAPK cascade. First, the concentrations of the phosphorylated kinases are denoted as

$$\begin{aligned}x_{11} &= [\text{Raf}^*], \\x_{21} &= [\text{MEK-P}], \\x_{22} &= [\text{MEK-PP}], \\x_{31} &= [\text{ERK-P}], \\x_{32} &= [\text{ERK-PP}].\end{aligned}$$

Since it is possible to compute the unphosphorylated inactive kinases Raf, MEK and ERK via conservation laws, it is not necessary to include them as state variables into the model. The conservation laws are given by

$$\begin{aligned}[\text{Raf}] + x_{11} &= x_{1t}, \\[\text{MEK}] + x_{21} + x_{22} &= x_{2t}, \\[\text{ERK}] + x_{31} + x_{32} &= x_{3t},\end{aligned}$$

where x_{1t} , x_{2t} and x_{3t} are parameters for the total concentrations of kinases. The time dependent behavior of the MAPK cascade is described by a set of differential equations derived from the reaction scheme shown in Figure 1 as follows.

$$\begin{aligned}\dot{x}_{11} &= v_1 - v_2 \\ \dot{x}_{21} &= v_3 + v_5 - v_4 - v_6 \\ \dot{x}_{22} &= v_4 - v_5 \\ \dot{x}_{31} &= v_7 + v_9 - v_8 - v_{10} \\ \dot{x}_{32} &= v_8 - v_9\end{aligned}\tag{31}$$

The rate equations v are given in Table 1. The numbers correspond to the labels in Figure 1. The slight modification which was made, compared to the model given in [11], is in the first rate equation in which a delay is introduced to the state variable x_{32} .

This model has 20 parameters and 1 delay, which is treated as a parameter as well. The nominal parameters are shown in the Table 2 and are taken from [11]. It should be noted that this model with the parameters defined in Table 2 does not show any oscillations. Instead, it has a stable equilibrium \bar{x}_1 and solutions converge to the steady state. The aim is now to show that by using the algorithm developed in the previous section the parameters and the delay can be varied leading to a change in stability. To this end, a loop breaking is defined at the point where the delay occurs, i.e. at the inhibitory feedback from the third level of the cascade to the first one. In the open loop system, the rate equation v_1 changes then to

$$v_1^{(ol)} = V_1 \frac{x_{1t} - x_{11}}{(1 + u/K_i)(K_{m1} + x_{1t} - x_{11})}.$$

Table 1: Rate equations for the MAPK cascade model (31).

Rate	Equation
v_1	$V_1 \frac{x_{1t} - x_{11}}{(1+x_{32}(t-\tau)/K_i)(K_{m1}+x_{1t}-x_{11})}$
v_2	$V_2 \frac{x_{11}}{K_{m2}+x_{11}}$
v_3	$k_3 x_{11} (x_{2t} - x_{21} - x_{22})$
v_4	$k_4 x_{11} x_{21}$
v_5	$V_5 \frac{x_{22}}{K_{m5}+x_{22}}$
v_6	$V_6 \frac{x_{21}}{K_{m6}+x_{21}}$
v_7	$k_7 x_{22} (x_{3t} - x_{31} - x_{32})$
v_8	$k_8 x_{22} x_{31}$
v_9	$V_9 \frac{x_{32}}{K_{m9}+x_{32}}$
v_{10}	$V_{10} \frac{x_{31}}{K_{m10}+x_{31}}$

Correspondingly, the loop breaking uses the output function

$$h(x(t - \tau)) = x_{32}(t - \tau).$$

As a next step, the linearization of (31) has to be obtained. From the linearization the transfer function $G(\xi, s, \tau)$ is derived. The aim is now to find new parameter p_2 and a new delay τ_2 for which the corresponding equilibria are not topologically equivalent.

4.2 Results of the MAPK cascade analysis

As the first step the critical frequency branch which is considered in the analysis has to be selected. It is suggested here that the frequency which is nearest to the point $G = 1$ is selected. By taking this frequency it is guaranteed that the computation time to find a change in stability is minimal since a change in stability is found by forcing this intersection to move from $G(\bar{\xi}, j\omega_c^{(i)}) < 1$ to $G(\bar{\xi}, j\omega_c^{(i)}) > 1$ or the other way around.

In the analysis, we compare two case studies with a different starting value of the delay: Case 1 uses $\tau = 10$ s, whereas Case 2 uses $\tau = 300$ s. In both cases, the algorithm is successful in finding a parameter vector for which sustained oscillations emerge. The resulting parameter values for the two cases are given in Table 2, and are discussed in more detail in the following sections. As a general point, it is observed that some parameters change only very slightly, while others change by up to 85 %. Due to the nature of the gradient-directed continuation algorithm, it can be concluded that the parameters where a larger change is observed have a higher influence on the occurrence of sustained oscillations, compared to the other parameters. Also observe that for almost all parameters, the direction of the change in the parameter value is independent of the value of the time delay, indicating that these parameters affect the existence of oscillations in a qualitatively consistent manner for different time delays.

Table 2: Nominal and perturbed parameter values for the MAPK cascade model

Param.	p_1	p_2 , Case 1	p_2 , Case 2	Unit
τ		10.2343	313.8295	s
V_1	2.5	1.4901	2.6791	nM/s
K_i	9	5.2438	9.4503	nM
K_{m1}	10	10.1921	10.0506	nM
V_2	0.25	0.0460	0.2375	nM/s
K_{m2}	8	2.7392	6.6321	nM
k_3	0.001	0.0012	0.0011	1/(s nM)
k_4	0.001	0.0008	0.0011	1/(s nM)
V_5	0.75	0.3891	0.6722	nM/s
K_{m5}	15	3.0475	9.7977	nM
V_6	0.75	1.3908	1.0945	nM/s
K_{m6}	15	12.6621	13.8714	nM
k_7	0.001	0.0003	0.0006	1/(s nM)
k_8	0.001	0.0009	0.0010	1/(s nM)
V_9	0.5	0.4449	0.5126	nM/s
K_{m9}	15	14.8553	14.8626	nM
V_{10}	0.5	0.7860	0.6849	nM/s
K_{m10}	15	12.4946	13.7226	nM
x_{1t}	100	104.0892	102.7038	nM
x_{2t}	300	401.6220	367.0280	nM
x_{3t}	300	422.2445	345.3910	nM

4.2.1 Case 1: $\tau = 10$ s

In this case, the critical frequency branch $\bar{\omega}_c$ is the one farthest to the right on the imaginary axis. After applying some iterations for a selected $\bar{\omega}_c$, the Newton-method results in $\omega_c^{(0)} = 0.0153 \text{ s}^{-1}$. The corresponding transfer function value is $\gamma(\omega_c^{(0)} = 0.0153 \text{ s}^{-1}) = 0.1501$, corresponding to the equilibrium \bar{x}_1 being stable in the closed loop system.

The final transfer function value at the critical frequency is $\gamma(\bar{\omega}_c) = 3.5954$, which is reached after 20 iterations of the algorithm. The delay changes by 2%, but other parameters change up to 85%, e.g. V_6 .

4.2.2 Case 2: $\tau = 300$ s

In this case, we again consider the critical frequency branch $\bar{\omega}_c$ which is farthest to the right on the imaginary axis. After applying some iterations for a selected $\bar{\omega}_c^{(0)}$, the Newton-method results in $\omega_c^{(i)} = 0.0051 \text{ s}^{-1}$. The corresponding transfer function value is $\gamma(\omega_c^{(i)} = 0.0051 \text{ s}^{-1}) = 0.6950$, corresponding to the equilibrium \bar{x}_1 being stable in the closed loop system.

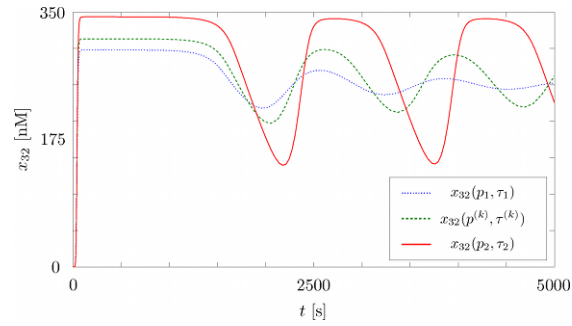
The final value is $\gamma(\bar{\omega}_c) = 1.7877$, as shown in Figure 2(b), which is reached after 18 iterations. In this experiment not all the parameters change throughout the analysis. The delay changes by 4%, but other parameters change up to 40%, e.g. k_7 . Trajectories of the perturbed system and the Nyquist plot for three selected parameters and delay found during the bifurcation search are displayed in Figure 2.

5 SUMMARY AND CONCLUSIONS

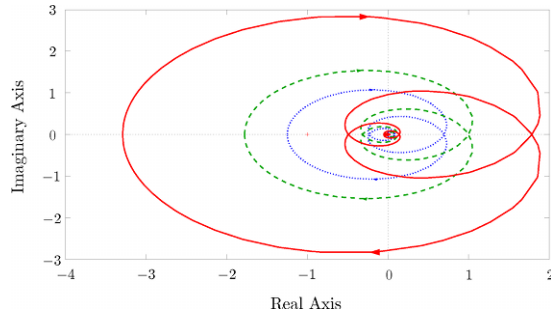
In this paper, the loop breaking approach for bifurcation search, originally presented in [11] for ordinary differential equations, is extended to time delay systems. While the basic idea is the same as in the previous case [11], the fact that the transfer function of a time delay system has an infinite number of crossings with the real axis requires a different approach to the computation of critical frequencies. Then, based on an analytical characterization of critical points in these systems, we develop an algorithm which allows to systematically search specifically for either static or dynamic bifurcations in a potentially high-dimensional parameter space.

Although the method has been formulated for systems with a single time delay only in this paper, it is also directly applicable to systems with multiple time delays, if the transfer function can be written as in (14). This is for example the case if multiple delays are situated along one signal flow path in the system without further intertwined feedback loops.

The developed method is particularly useful for biochemical systems, where many parameters are uncertain and may be subject to variations. In the paper, we illustrate the benefits of the proposed methods by applying it to a model of a MAPK cascade, which is a frequent module in biochemical signaling pathways.



(a)



(b)

Figure 2: Solutions and nyquist plot for Case 2 ($\tau = 300$ s) Dotted line corresponds to starting parameter values p_1 , dashed line to intermediate parameter values during the bifurcation search, and full line to final parameter values p_2 .

In this case study, our algorithm is able to determine a variation in the parameter values which leads to the emergence of sustained oscillations. By the nature of the gradient-directed continuation algorithm, it is also possible to evaluate which parameters are most relevant for the occurrence of the considered change in the dynamical behavior.

References

- [1] L. Dugard and E. I. Verriest. *Stability and Control of Time-delay Systems*. Springer, 1998.
- [2] K. Gu, V. L. Kharitonov, and J. Chen. *Stability of Time-Delay Systems*. Birkhaeuser, Boston, 2003.
- [3] C. Y. Huang and J. E. Ferrell. Ultrasensitivity in the mitogen-activated protein kinase cascade. *Proc. Natl. Acad. Sci.*, 93(19):10078–83, Sep 1996.
- [4] B. N. Kholodenko. Negative feedback and ultrasensitivity can bring about oscillations in the mitogen-activated protein kinase cascades. *Eur. J. Biochem.*, 267(6):1583–88, Mar 2000.
- [5] T. Kobayashi, L. Chen, and K. Aihara. Modelling genetic switches with positive feedback loops. *Journal of Theoretical Biology*, 221:379–399, 2002.
- [6] A. M. Krall. Stability criteria for feedback systems with a time lag. *SIAM J. Contr. Optim.*, 2:160–170, 1964.
- [7] Y. A. Kuznetsov. *Elements of Applied Bifurcation Theory*. Springer-Verlag, New York, 1995.
- [8] M. Mincheva and M. R. Roussel. Graph-theoretic methods for the analysis of chemical and biochemical networks. II. Oscillations in networks with delays. *J Math Biol*, 55(1):87–104, Jul 2007.
- [9] N. A. M. Monk. Oscillatory expression of Hes1, p53, and NF-kappaB driven by transcriptional time delays. *Curr Biol*, 13(16):1409–1413, Aug 2003.
- [10] U. Münz, C. Ebenbauer, T. Haag, and F. Allgöwer. Stability analysis of time-delay systems with incommensurate delays using positive polynomials. *IEEE Trans. Autom. Control*, 54(5):1019–1024, May 2009.
- [11] S. Waldherr and F. Allgöwer. Searching bifurcations in high-dimensional parameter space via a feedback loop breaking approach. *Int. J. Syst. Sci.*, 40:769–782, 2009.
- [12] O. Wolkenhauer, M. Ullah, P. Wellstead, and K.-H. Cho. The dynamic systems approach to control and regulation of intracellular networks. *FEBS Lett*, 579(8):1846–1853, Mar 2005.

- [13] Q. Zhong. *Robust Control of Time-delay Systems*. Springer-Verlag, Liverpool, 2006.